Journal of Quantitative Spectroscopy & Radiative Transfer 187 (2017) 443–452

Contents lists available at ScienceDirect

Journal of Quantitative Spectroscopy & Radiative Transfer

journal homepage: www.elsevier.com/locate/jqsrt

Optical properties of black carbon aggregates with non-absorptive coating

Chao Liu [a,b,*], Ji Li [a,b], Yan Yin [a,b], Bin Zhu [a,b], Qian Feng [c]

[a] Collaborative Innovation Center on Forecast and Evaluation of Meteorological Disasters, Nanjing University of Information Science & Technology, Nanjing 210044, China

[b] Key Laboratory for Aerosol-Cloud-Precipitation of China Meteorological Administration, School of Atmospheric Physics, Nanjing University of Information Science & Technology, Nanjing 210044, China

[c] National Satellite Ocean Application Services, Beijing 100081, China

ARTICLE INFO

Article history:
Received 29 September 2016
Received in revised form
28 October 2016
Available online 5 November 2016

Keywords:
Black carbon
Coating
Optical properties

ABSTRACT

This study develops an idealized model to account for the effects of non-absorptive coating on the optical properties of black carbon (BC) aggregates. The classic fractal aggregate is applied to represent realistic BC particles, and the coating is assumed to be spherical. To accelerate the single-scattering simulation, BC monomers that were overlapped with coating sphere (not those completely inside the coating) are slightly moved to avoid overlapping. The multiple-sphere T-matrix method (MSTM) becomes applicable to calculate the optical properties of inhomogeneous particles with any coating amount, and is generally two orders of magnitude faster than the discrete-dipole approximation for particles we considered. Furthermore, the simple spherical coating is found to have similar effects on the optical properties to those based on more complicated coating structure. With the simple particle model and the efficient MSTM, it becomes possible to consider the influence of coating with much more details. The non-absorptive coating of BC aggregates can significantly enhance BC extinction and absorption, which is consistent with previous studies. The absorption of coated aggregates can be over two times stronger than that of BC particles without coating. Besides the coating volume, the relative position between the mass centers of BC aggregate and coating also plays an important role on the optical properties, and should obviously be considered in further studies.

1. Introduction

Black carbon (BC, or soot), emitted from incomplete combustion of fossil fuel, biofuel and biomass, is one of the strongest absorptive aerosols for solar radiation [1–4]. Once emitted into the atmosphere, BC particles quickly become inhomogeneous during the aging processes [5,6]. BC and its mixtures influence local and global climate directly by strongly absorbing the solar radiation [7,8]. Due to complex geometry and mixing structure, our understanding on BC optical properties is still limited [9], which makes BC, especially aged BC, one of the largest uncertainties in estimating aerosol radiative forcing [10–12].

BC particles normally exist in the atmosphere as aggregates with a large number of small spherical particles, and show really complex overall geometries [13]. Observations indicate that, during the aging process, BC aggregates with open cluster structures may collapse and become compact [14,15]. Meanwhile, those aggregates can mix with other aerosol components by absorption or condensation of gaseous species, coagulation with other aerosols and oxidation [7,16], and become inhomogeneous with coatings of water, sulfate or other non-absorptive materials [17]. With the significant variation on particle geometry and component, the optical properties of BC aggregates can be quite different during the aging. Both laboratory and numerical studies show that the absorption and scattering of BC aerosols can be greatly enhanced after coating or hygroscopic growth [5,18,19]. The enhancement leads to systematic errors in interpreting measurements of ambient BC concentrations [20], and brings significant uncertainties on estimating its radiative effects [21,22].

Numerical modeling becomes one of the most fundamental and important methods to improve our understanding on the effects of coating on BC optical properties. For homogeneous BC particles, the fractal aggregate is the most successful model to represent realistic particle geometries, and is widely accepted to estimate their optical properties [23,24]. However, due to the

* Corresponding author at: Collaborative Innovation Center on Forecast and Evaluation of Meteorological Disasters, Nanjing University of Information Science & Technology, Nanjing 210044, China.
E-mail address: chao_liu@nuist.edu.cn (C. Liu).

http://dx.doi.org/10.1016/j.jqsrt.2016.10.023
0022-4073/

uncertainty and complexity on coated BC particles, quite different models with both simple and complex geometries were built [4,23–28]. The simplest models treat inhomogeneous particles as homogeneous ones by applying the effective medium approximations [2,19,29]. The core-shell spherical model, simplest inhomogeneous model, is also widely used, because the scattering properties can be easily given by the core-shell Mie theory [25,30,31,32]. However, those simple geometries are significantly different from the realistic particles. Meanwhile, some non-spherical and inhomogeneous models are built to give a better representation on particle geometries. Liu et al. add thin water film independently to each monomer, and consider fractal aggregate with core-shell monomers [30]. Dong et al. [25] and Liu et al. [29] introduce 'irregular' coating to fractal aggregates, and use the discrete dipole approximation (DDA) to calculate their optical properties. Those models do build numerical particles quite close to realistic ones, whereas the corresponding calculation for the optical properties is neither simple nor efficient. Thus, this study intends to develop a model that can not only better represent real coated BC particles but also be efficiently considered for light scattering simulations.

To further improve our understanding on the optical properties of aged BC, we build a simple model to account for the effects of non-absorptive coating on their optical properties. The paper is organized as follows. Section 2 introduces the model to represent inhomogeneous BC particles, and the numerical models to calculate their optical properties are compared. The effects of coating on BC optical properties are discussed in Section 3, and Section 4 concludes this work.

2. BC aggregates with coating and their optical properties

The geometry of homogeneous BC is normally constructed following the well-known framework of the fractal aggregate, and it describes BC particles using the statistical scaling rule [33]:

$$N = k_f\left(\frac{R_g}{a}\right)^{D_f} \tag{1}$$

where N is the number of monomers in an aggregate, and a is the monomer radius. k_f and D_f are the fractal prefactor and fractal dimension, respectively, and they indicate the overall structure of the aggregates. R_g, the gyration radius, is defined as a measure of the aggregate overall spatial size, and it can be calculated by

$$R_g^2 = \frac{1}{N}\sum_{i=1}^{N}(\boldsymbol{r_i} - \boldsymbol{r_0})^2 \tag{2}$$

where $\mathbf{r_i}$ is the position vector of the ith monomer center, and $\mathbf{r_0}$ indicates the position vector of the aggregate mass center. As D_f or k_f increases, the aggregate tends to be more compact. For example, aggregates with D_f close 1 correspond to those with a lacy chain-like structure, and compact aggregates have D_f almost 3. We keep using the fractal aggregates to define homogeneous BC particles. This study fixes the values of k_f and a to be 1.2 and 15 nm, respectively, which are both typical observed values [33]. To represent fresh (lacy/open clusters) and aged (compact particles) BC aggregates, we consider two D_f values of 1.8 and 2.8 for comparison [16,26]. A tunable particle-cluster aggregation algorithm is used to generate aggregates with given geometric parameters (N, a, D_f, and k_f) [27,34–36].

The geometries of fractal aggregates are widely applied, whereas models for coated ones are still under discussion. Some models oversimplify particle geometries for the sake of computational convenience [30,35,36]. Meanwhile, some complex geometries are developed to represent realistic particles, whereas the computational burden for the single-scattering simulation limits the applications of those models [25,29]. To build a realistic particle model for efficient optical simulation, the simplest three-dimension geometry, sphere, is "coated" to the soot fractal aggregate. Actually, some microscopic images of aged BC particles do show spherical coating geometry [16,25].

To form an inhomogeneous particle, we first generate a fractal aggregate and a spherical coating with given sizes separately. Secondly, the coating sphere is randomly placed "in the aggregate" with a given distance between their mass centers. It should be noticed that the coating sphere should be enlarged to offset the volume occupied by the monomers inside and to reach the required coating volume. Last, the BC monomers that are completely inside or outside of the coating sphere are kept, whereas those that are partially inside and partially outside (overlapping) are slightly moved to the outside of the coating sphere. Therefore, we can generate such an inhomogeneous BC particle with only spherical elements but without overlapping ones, and both aggregate and coating sizes can be arbitrary. The size of BC aggregate, i.e. N, and the volume fraction of the BC aggregate or coating to the inhomogeneous particle, i.e. f_{BC} or $f_{coating}$, are used to specify particle overall 'size'. $f_{coating}$ is given by:

$$f_{coating} = 1 - f_{BC} = \frac{V_{coating}}{V_{coating} + V_{BC}} \tag{3}$$

where V_{BC} and $V_{coating}$ are the volume of the BC aggregate and coating, respectively.

The 2D images in Fig. 1 show the typical examples of monomer movements to avoid overlapped spheres. The gray and blue spheres represent BC monomers and coating, respectively, and the red spheres indicate the moved monomers. The left and middle panels show 2D particles before and after the move. The top row is for an aggregate with relatively lacy structure (e.g., D_f=1.8), and, with enough space outside the coating sphere, we can simply move the overlapped monomers to the outside and to be attached with the coating sphere. For aggregates with compact structure (e.g., D_f=2.8), the outside of the coating sphere is mostly occupied by other monomers, and we may move the monomers outward until all overlapping avoided. This is illustrated by the 2D images in the bottom row of Fig. 1. Considering the small monomer size (radius of 15 nm in this study), the distance moved to avoid overlapping is small compared with the wavelength we consider (i.e., 550 nm). The influence of such movement on optical

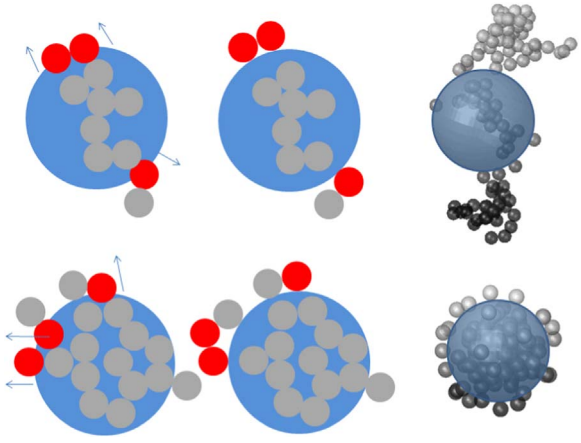

Fig. 1. Procedures to generate a fractal aggregate with a spherical coating and no overlapping monomers, and two examples of coated BC aggregates (100 monomers) with fractal dimension of 1.8 and 2.8. Gray and blue spheres represent BC and coating, respectively, and the red ones are the moved monomers. (For interpretation of the references to color in this figure legend, the reader is referred to the web version of this article.)

properties will be discussed. The right panels of Fig. 1 show two examples of final coated BC aggregates. The fractal aggregates both compose 100 monomers, and have D_f of 1.8 (top) and 2.8 (bottom). The coating size is determined to make coating volume fraction $f_{coating}$ to be 0.5. The numerical particles show quite similar geometries to those realistic coated BC [16]. It should be noted that similar models with spherical host and BC inclusions or attached BC (i.e. inside or outside host spheres) were also investigated by [23,35,37,38], and various important conclusions were drew from different aspects. This work generalizes the model to provide a more systematic investigation, and focuses on the effects of coating on BC optical properties.

By using a spherical coating and avoiding overlapped spheres, this study takes the advantage of the multiple-sphere T-matrix method (MSTM), which is one of the most efficient and accurate model to calculate the optical properties of a cluster of spheres without overlapping [39,40]. To demonstrate the efficiency of the MSTM, we briefly compare the MSTM and DDA methods for light scattering of coated BC particles. The MSTM employs the addition theorem of vector spherical wave functions to account for mutual interactions among the system, and the T-matrix of multiple spheres can be obtained from those of individual spheres [39]. All information required for particle optical properties can be derived from its T-matrix. Different from most other numerically exact models, the MSTM calculates the optical properties of randomly oriented particles analytically without numerical averaging over particle orientations, and the scatterer is defined accurately by the positions and sizes of the spherical elements. The popular and robust MSTM code that is widely applied to obtain the optical properties of fractal aggregates will be used in this study [27,38,40–42]. Meanwhile, the DDA is a powerful method to calculate scattering and absorption of electromagnetic waves by arbitrarily shaped particles. For the DDA, the particle is discretized into small cubical sub-volumes (namely dipoles), and the interactions of dipoles are approximated based on the integral equation for the electric field. To account for the optical properties of randomly oriented particles, the DDA has to be applied multiple times for averaging over different particle orientations, whereas only one simulation is needed for the MSTM. The Amsterdam-DDA is used in this study [43–45]. Both the MSTM and DDA implementations are parallelized, and can be carried out on multiple processors.

This study considers an incident wavelength of 550 nm. The BC refractive index of $1.73+0.59i$ is used following [46,47]. The coating is assumed to be non-absorptive material with a refractive index of $1.43+0i$, and the value is close to that of sulfate and other inorganic aerosols [25]. To avoid the influence of random aggregation geometry and monomer movement, results for each case with given parameters are averaged over those from five different particle realizations. The results discussed in this study can be generally understood as the influence of non-absorptive coating on BC optical properties. We will discuss both the integral scattering properties (including the extinction cross section C_{ext}, absorption cross section C_{abs}, single-scattering albedo *SSA*, and asymmetry factor g) and the angular-dependent scattering matrix $\boldsymbol{P}$.

Table 1 compares the efficiency of the MSTM and DDA for light scattering simulation of homogeneous and coated aggregates. Because the computational times used by both methods are highly sensitive to particle size and geometry, only four extreme cases are discussed, i.e., lacy and compact aggregates (D_f=1.8 and 2.8) without coating or with a large spherical coating. The computational times of the four cases used by the MSTM and DDA method as well as their geometries are given in the table. Both methods are carried out using a single node with 24 64-bit 2.5 GHz processors. Aggregates with 200 monomers are considered, and the coating volume fraction is $f_{coating}$=0.99 for the coated cases. For the DDA simulations, particles are discretized by grids with 80

Table 1
Computational time (in seconds) of the MSTM and DDA method for BC aggregates with and without coating sphere.

D_f	Method	$f_{coating}$=0.0	$f_{coating}$=0.99
1.8	Geometry		
	MSTM	16.35	5.18
	DDA	179.63	243.35
2.8	Geometry		
	MSTM	8.16	6.10
	DDA	3.77	226.23

dipoles per wavelength, and such a fine resolution is used to capture the small monomer geometry (e.g., each monomer is represented by approximately 40 dipoles). At D_f =1.8, the MSTM is more than 10 times faster than the DDA. As the homogeneous aggregate becomes compact, both the MSTM and DDA can be done in a few seconds. With a heavy coating added ($f_{coating}$=0.99), the MSTM becomes even more efficient, whereas the DDA takes over two hundred seconds to finish the simulation, which is over 30 times slower than the MSTM. The advantage of the MSTM will be more significant as the aggregate or coating size increases. Table 1 generally shows the relative efficiencies of the two models for light scattering simulations of this study, and, with the MSTM almost two orders of magnitude faster than the DDA, it becomes convenient to study the influence of non-absorptive coating in much more details.

It should be noticed that the MSTM results can be understood as the numerically exact solution for clusters of spheres. However, the DDA may introduce errors due to definition of particle geometry and average over particle orientations, and its accuracy on inhomogeneous particles is also limited [48]. To show the accuracy of the two models, Table 2 compares the optical properties of coated aggregates with 200 monomers and a coating volume fraction of 0.5. The values in the parentheses are the relative differences of the DDA results (both DDA I and DDA II) compared to the MSTM results. The DDA I considers coated aggregates without overlapping, which is exactly the same particle modeled by the MSTM, and, thus, the comparison between the MSTM and DDA I indicates the relative errors given by the DDA model. The errors are under 4%, and becomes even smaller for compact aggregates. The errors here have similar magnitude to those of the DDA for core-shell spheres given by Liu et al. [48]. As discussed above, this study moves some of the aggregate monomers slightly to avoid overlapping, and the influence of such movement is demonstrated in Table 2. For the DDA II, we consider aggregates with coating added but without moving overlapped monomers, and, thus, the comparison between the DDA I and DDA II can indicate the influence of the movement on BC optical properties. Most integral scattering properties of the DDA I and DDA II are close to each other. The small relative differences introduced by moving some monomers to the outside of coating can definitely be ignored, because similar errors may be introduced by the single-scattering simulations or by the significant uncertainties on BC geometries. Furthermore, the differences in the scattering matrix elements are even smaller, and we are not shown here. This study mainly takes the advantage of the efficiency provided by the MSTM, whereas its higher accuracy compared to the DDA is not really critical due to the uncertainty on the geometry of BC coating. More detailed comparison between the two models can be found in [42].

Table 2
Integral optical properties of coated BC aggregates given by the MSTM and DDA. The aggregate has 200 monomers, and the coating volume fraction is 0.5.

Model	$D_f = 1.8$				$D_f = 2.8$			
	C_{ext} ($\times 10^{-2}\mu m^2$)	C_{abs} ($\times 10^{-2}\mu m^2$)	*SSA*	*g*	C_{ext} ($\times 10^{-2}\mu m^2$)	C_{abs} ($\times 10^{-2}\mu m^2$)	*SSA*	*g*
MSTM	3.8	2.8	0.26	0.46	5.1	3.1	0.39	0.41
DDA I[a]	3.9(2.6%)	2.9(3.4%)	0.26(0%)	0.45(-2.2%)	5.2(2.0%)	3.2(3.2%)	0.39(0%)	0.41(0%)
DDA II[b]	4.0(5.3%)	2.9(3.4%)	0.27(3.9%)	0.45(-2.2%)	5.3(3.9%)	3.3(6.5%)	0.38(-2.6%)	0.39(-4.8%)

[a] The geometry defined by the DDA is the aggregate with spherical coating added, and the overlapping between the aggregate monomers and coating is removed.
[b] The geometry defined by the DDA is the aggregate with spherical coating added, whereas the overlapping between the aggregate monomers and coating is not removed.

In conclusion, the inhomogeneous BC model is defined based on the fractal aggregate and spherical coating, and quite realistic geometries are generated with great flexibility. With overlapped monomers avoided, the MSTM model is used to calculate the single-scattering properties, and the efficiency of the MSTM makes it possible to study the influence of coating on BC optical properties with more details.

3. Influence of non-absorptive coating on BC optical properties

This study focuses on the influence of non-absorptive coating on BC optical properties, and, thus, the properties of the coating are our interest. With coating geometry fixed, we will consider the other two factors: coating volume and relative position between the aggregate and coating.

To show the influence of coating volume, we consider particles with a fixed aggregate size, and increase coating amount. Starting from homogeneous aggregates with 200 monomers, Fig. 2 illustrates the geometries of coated BC with different coating fraction $f_{coating}$. The fractal dimensions of the aggregates are 1.8 and 2.8, and the coating fraction $f_{coating}$ are 0.5, 0.75 and 0.99. The relative distance between the centers of aggregate and coating is set to be 0. The gray spheres in the figure are BC monomers, and the transparent blue one is the coating. As the coating volume increases, the particle overall geometry becomes a sphere with BC aggregate inside. When $f_{coating}$ reaches 0.9, the compact aggregate with a D_f of 2.8 can be completely included in the coating sphere. However, for the lacy aggregate with D_f=1.8, the coating fraction has to be increased to almost 0.99 to contain all BC monomers, and the corresponding radius of the coating sphere is over 25 times larger than that of a BC monomer.

Fig. 3 illustrates the optical properties of coated BC as a function of the coating volume added to the BC aggregates. The coating volume is given in unit of the original aggregate volume, and the largest coating volume in the figure (99 times of the corresponding aggregate volume) gives a coating fraction of 0.99. It is expected that, as the coating volume increases, C_{ext} becomes much stronger. With $f_{coating}$ reaching 0.99, the projected area becomes approximately 7 times larger than that of the original BC aggregates, whereas the extinction cross sections become almost 70 times larger from 0.03 μm^2 to over 2 μm^2. Although the volume of the absorptive material (i.e. BC) is fixed, the absorption of the coated particles also shows a clear increase. For the lacy aggregates, the absorption cross section keeps increasing even if the coating fraction increases to 0.99, whereas, for compact aggregates, the absorption stops increasing after the coating volume reaching to approximately 20 times of aggregate volume. The absorption can reach a maximum of over 2 times that of the homogeneous aggregates with 200 monomers. For aggregates with different geometries, the compact aggregates are more absorptive without coating or with thin coating, and the lacy ones absorb more with heavy coating. With non-absorptive coating considered, aggregates show a much stronger scattering enhancement than absorption, and, thus, the *SSA* increases from approximately 0.2 to 0.8 as $f_{coating}$ increases to 0.9. The asymmetry factor *g* increases from 0.4 to almost 0.8 for heavily coated particles, mainly due to the increase of particle volume. It should be noticed that, for the extreme cases with coating fraction close to 1, the optical properties are close to that of the non-absorptive sphere, and the BC mainly affects the absorption. We also find that the influence of our spherical coating on BC optical properties have similar magnitude to those with more complex coating structures [25,29], and the details will not be given here.

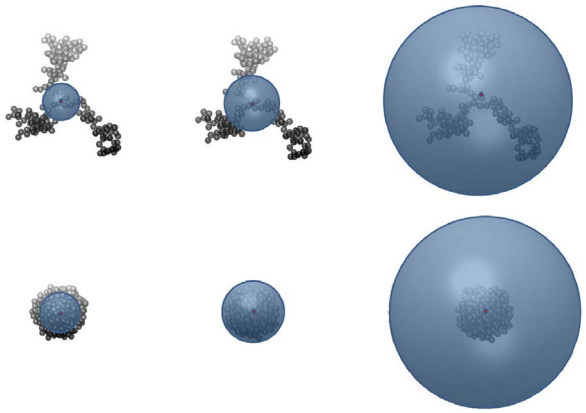

Fig. 2. Some examples of coated fractal aggregates with 200 monomers. The coating fractions from left to right are 0.5, 0.75, and 0.99.

The influence of coating on the scattering matrix of BC aggregates was seldom discussed. Fig. 4 shows the normalized phase function and other non-zero matrix elements of coated aggregates with a fractal dimension of 1.8 and coating fractions of 0, 0.5, 0.75, 0.9 and 0.99. The phase functions are the most sensitive element to the amount of coating. When the coating volume is comparable to that of the BC aggregate, e.g., $f_{coating} < 0.75$, the forward scattering decreases as the coating fraction increases. This is because the forward peak of a small coating sphere is weaker than that of the lacy aggregate, and the phase function of the coated aggregate can be understood as 'an average' of those of the two (i.e., coating sphere and aggregate). When the coating becomes dominant, the forward peak increases as the coating fraction increases, and the phase function of heavily coated BC is close to that of the same-sized homogeneous coating sphere, which is illustrated in Fig. 4 (labeled as $f_{coating}$=1). The other scattering matrix elements of homogeneous BC aggregates show clear features of Rayleigh scattering (e.g. $P_{22}/P_{11}=1$, $P_{34}=0$), whereas the features disappear as the coating fraction becomes larger than 0.75. Thus, the polarization properties of the BC particles can be a potential characteristic to understand their coating and mixing state.

Fig. 5 is the same as Fig. 4 but for aggregates with a fractal dimension of 2.8, and the results are similar to those of aggregates

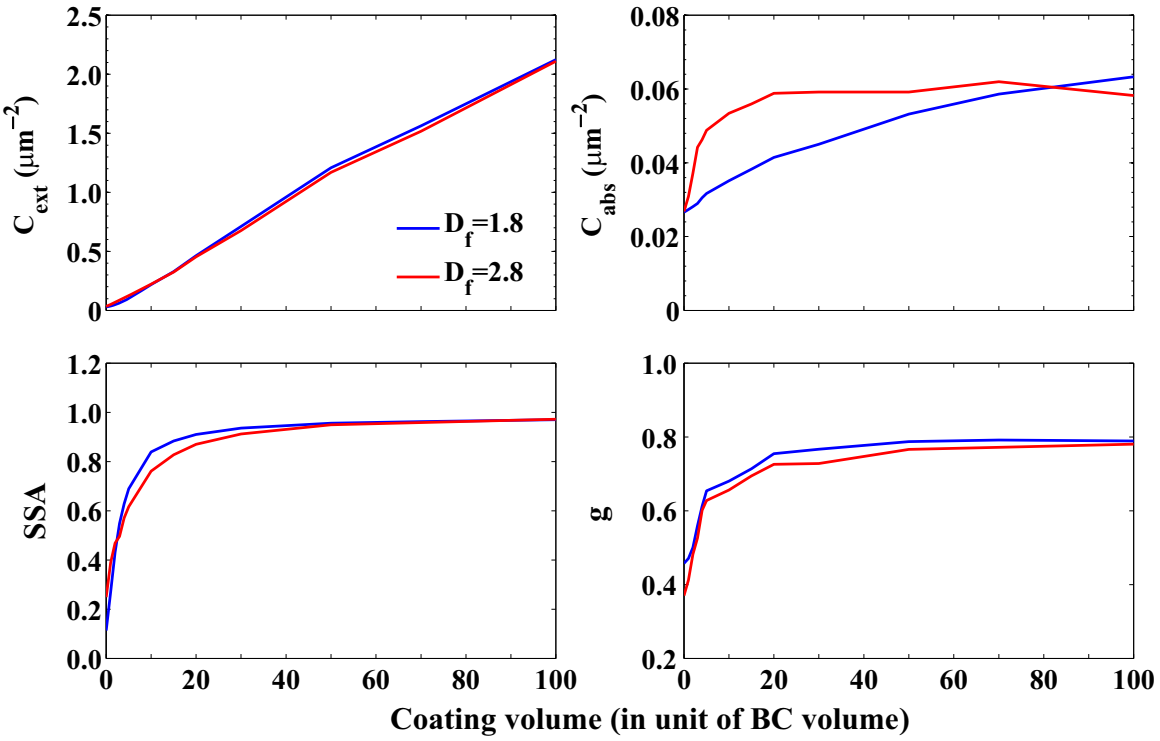

Fig. 3. Extinction cross section (C_{ext}), absorption cross section (C_{abs}), single scattering albedo (*SSA*) and asymmetry factor (g) of BC aggregates with 200 monomers as functions of coating volume fraction.

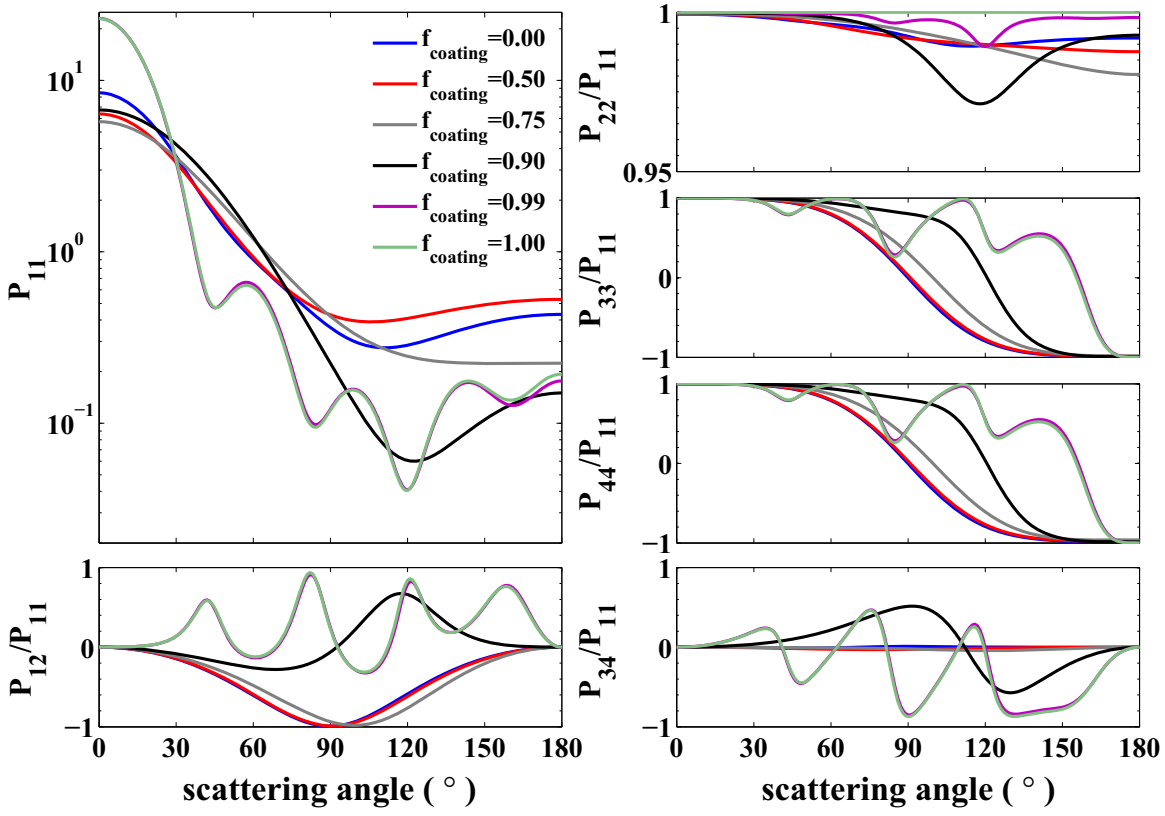

Fig. 4. Scattering matrix elements of BC aggregates with 200 monomers. The fractal dimension of the aggregates is 1.8, and the coating fractions of 0, 0.5, 0.9, 0.99 and 1.0 are considered.

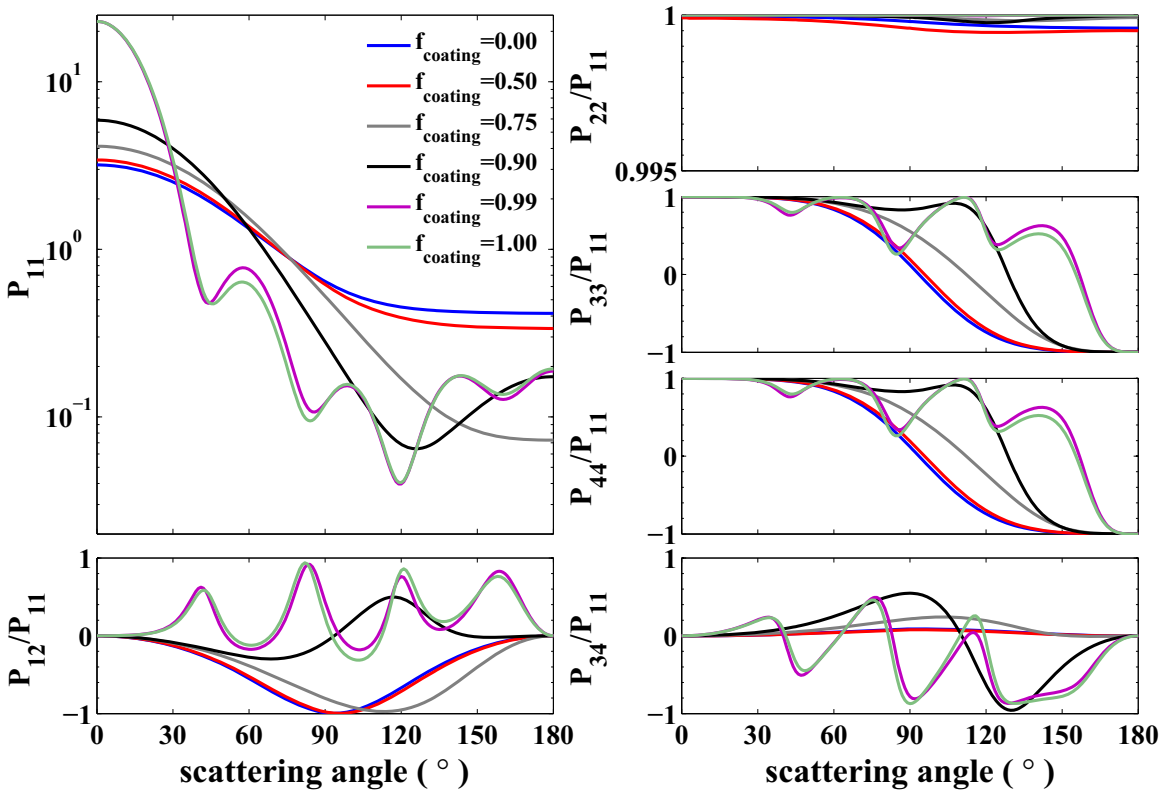

Fig. 5. Same as Fig. 4 but for aggregates with a fractal dimension of 2.8.

with D_f=1.8. Unlike the lacy aggregates, the forward peak for compact aggregates shown in Fig. 5 increases with the increase of coating fraction, when the coating fraction becomes larger than 0.5. Because the forward peaks in phase functions of a compact aggregate and a similar-sized sphere are similar, their average becomes larger if the sphere increases.

The simulations discussed above assume the centers of the non-absorptive coating and fractal aggregate to coincide, whereas this does not always stand for realistic particles. The relative position of mass centers of the fractal aggregate and coating can be arbitrary, which would be certainly true for realistic particles. Fig. 6 shows some examples of coated aggregates with 200 monomers and a coating fraction of $f_{coating}$=0.5, but particles with different relative distances are illustrated. We define distance between the mass centers of a fractal aggregate and a coating sphere as *d*, which is a variable to generate inhomogeneous particles. For the lacy aggregate in the top row, the distance *d* can be as large as 480 nm to keep the aggregate and sphere connected (right). When *d* reaches 240 nm, the compact aggregate and coating become separated. With different volume fractions, the maximum distances to keep the two materials connected are also different.

The integral scattering properties of coated aggregates are shown in Fig. 7 as functions of coating position *d*. Both lacy and compact aggregates with 200 monomers are considered, and the three columns correspond to particles with coating fractions of 0.5, 0.75 and 0.99. As mentioned above, we move the coating sphere from the aggregate center until it becomes untouchable with the aggregates, and the x-axis is for the relative distance between the centers of aggregate and coating sphere, i.e. *d*. It is evident that the integral optical properties are very sensitive to the coating position. When the coating volume is similar to that of aggregate (left and middle panels), the extinction and absorption both decreases as *d* increases, and the decrease is more significant for compact aggregates. If the coating becomes much heavier

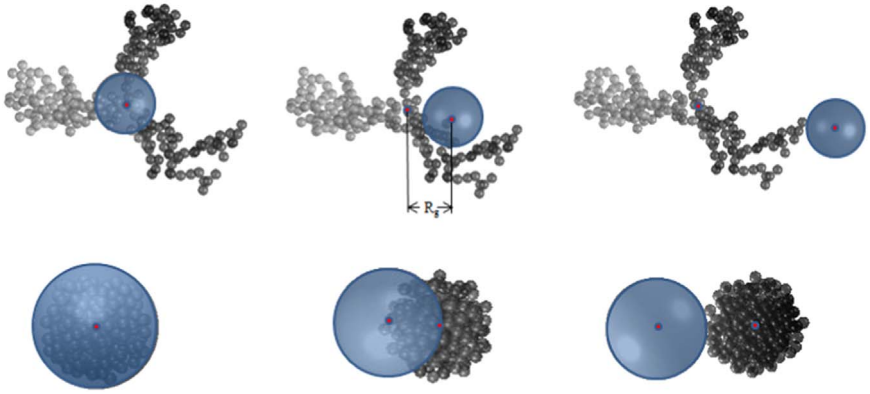

Fig. 6. Some examples of coated aggregates (200 monomers) with different distances between the aggregate and coating sphere.

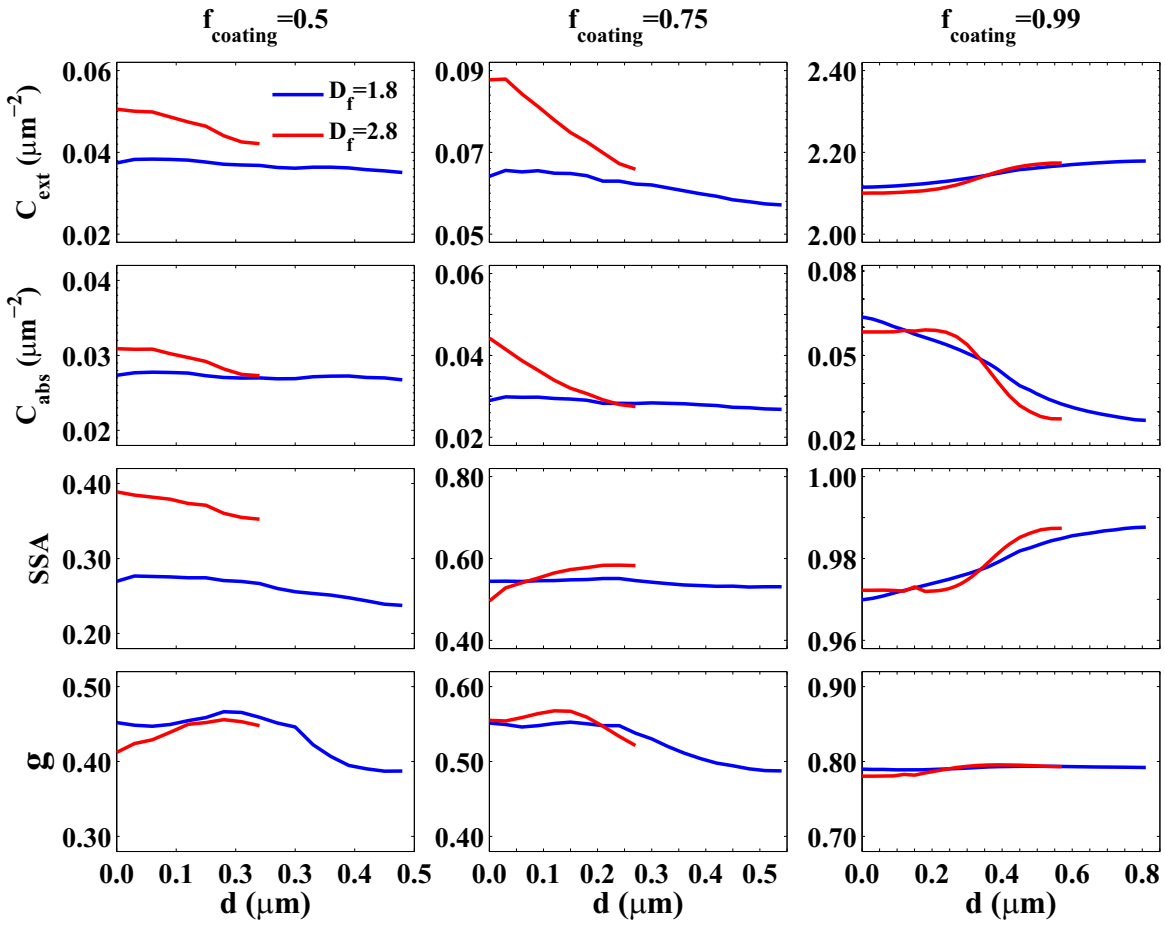

Fig. 7. Extinction cross section (C_{ext}), absorption cross section (C_{abs}), single scattering albedo (*SSA*) and asymmetry factor (g) of BC aggregate with 200 monomers and different coating positions.

($f_{coating}$=0.99), the extinction may increase as two elements (i.e., coating and aggregate) depart, whereas the decrease on the absorption becomes more significant. For coated aggregates with $f_{coating}$=0.99, the absorption decreases over 50% as the centers of the aggregate and coating departs, because the aggregate that is originally inside the coating sphere is moved to the outside. With the changes on the extinction and absorption discussed, the influence on the *SSA* can be easily understood. For $f_{coating}$=0.5, the *SSA* decreases as d becomes larger, whereas a slow increasing trend shows for particles with large $f_{coating}$. The influence on the asymmetry factor g seems more complicated, and this may be because of the significant changes on particle geometries at different d.

Fig. 8 compares the scattering matrix elements of coated aggregates with different relative coating positions. The results include those for coated aggregates with two coating fractions ($f_{coating}$=0.5 and 0.99) and three relative coating positions. For the three different relative positions, the coating spheres are located at the center, gyration radius and edge of the aggregates. It is evident that the phase function shows slight sensitivity to the relative positions between the coating and aggregate when the coating fraction is small. When the coating volume becomes much larger than that of the aggregate, the influence of position on the phase function can be ignored. Meanwhile, there is little difference on the other scattering matrix elements for coated aggregate with different coating positions.

Atmospheric applications interest in the bulk optical properties averaged over certain particle size distributions and this study consider an ensemble of aggregates with different sizes but the same coating fraction. The equivalent volume spheres of BC aggregates are assumed to follow a lognormal size distribution in the form of:

$$n(r) = \frac{1}{\sqrt{2\pi}\, r\ \ln(\sigma_g)} \exp\left[-\left(\frac{\ln(r) - \ln(r_g)}{\sqrt{2}\ \ln(\sigma_g)} \right)^2 \right],$$

where r_g and σ_g are the geometric mean radius and geometric standard deviation, respectively [20,43]. r is the radius of a sphere with the same volume as that of a fractal aggregate (i.e. equivalent volume sphere). We consider the size distribution of aggregates without coating with r_g of 0.06μm and σ_g of 1.5 [22,44], and aggregates with monomer sizes from N=25 to 1000 in steps of 25 are considered for the averaging. The formulas for the bulk property simulations can be found in [47]. To calculate the bulk properties, the coating fraction is fixed for each aggregate.

Table 3 compares the bulk optical properties of BC aggregates under different coating conditions, and results with coating fractions of 0, 0.5, 0.75, 0.9 and 0.99 are given. The distance between the aggregate and coating is 0. The results for bulk optical properties are similar to those of the single-sized aggregate as shown in Fig. 3 but with different magnitudes. The enhancement on the extinction is caused by the increase in particle volume, and is mainly contributed by the increase of scattering. The influence of coating on the absorption is quite sensitive to aggregate geometry. For the aggregates with D_f=1.8, the enhancement on absorption is weak when the coating fraction is small. This can be explained by

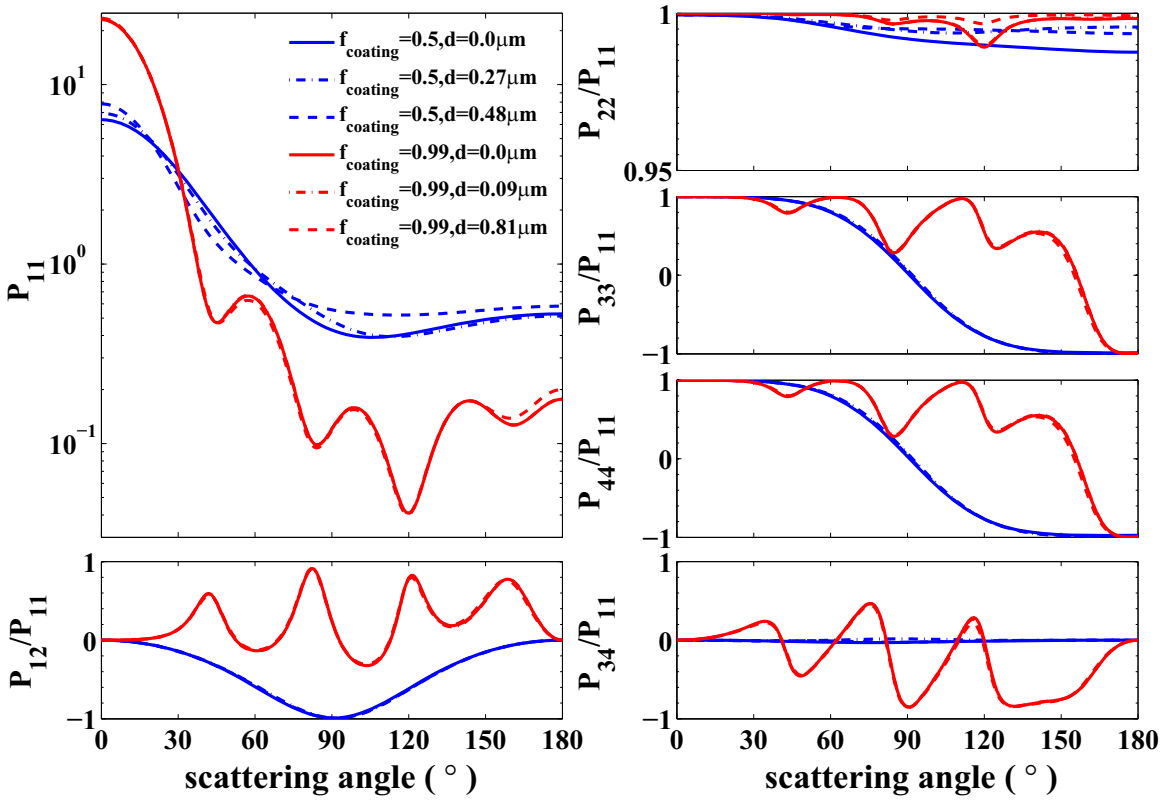

Fig. 8. Scattering matrix elements of BC aggregate with 200 monomers and non-absorptive coating, and the coating is located at the center, gyration radius and edge of the aggregate.

Table 3
Bulk optical properties of coated BC aggregates.

	D_f=1.8					D_f=2.8				
$f_{coating}$	0.00	0.50	0.75	0.90	0.99	0.00	0.50	0.75	0.90	0.99
C_{ext}($\times 10^{-2}\mu m^2$)	1.7	2.1	3.8	11	98	2.0	2.7	4.8	11	98
C_{abs}($\times 10^{-2}\mu m^2$)	1.5	1.5	1.6	1.8	3.5	1.5	1.6	2.4	2.8	3.5
SSA	0.12	0.30	0.58	0.83	0.96	0.25	0.41	0.51	0.74	0.96
g	0.54	0.55	0.62	0.70	0.76	0.50	0.54	0.58	0.67	0.75

the different trends of the two lines in the upper right panel of Fig. 3. The bulk absorption cross sections can be over two times larger as the coating fraction close to 1. For coated BC aggregates, when the volume fraction of the non-absorptive coating reaches to approximately 0.75, the scattering and absorption becomes comparable, i.e. *SSA* close to 0.5. The asymmetry factor also increases from 0.5 to over 0.75 for both lacy and compact aggregates.

The corresponding bulk scattering matrix elements of coated BC with different coating fractions are shown in Fig. 9, and the results are for aggregates with a fractal dimension of 1.8. The volume fractions of the coating used are the same as those for Fig. 4. As expected, the influence of the non-absorptive coating on the phase functions is similar to that for a single-sized particle (see Fig. 4). When the volume fraction of coating is small, the forward peak of the phase function decreases as the coating increases. After the coating fraction $f_{coating}$ becoming larger than 0.9, the forward peak becomes much stronger. For the other non-zero scattering matrix elements, the feature of the Rayleigh scattering becomes weak as the coating volume fraction becomes larger than approximately 0.75. Compared to the results shown in Fig. 4, the oscillations in the scattering matrix elements of Fig. 9 for particles with large coating spheres are smoothed out by the averaging over particle size distribution. The results for aggregates with compact structures are similar, and will not be given here.

4. Conclusion

This study develops a simple inhomogeneous model to study the optical properties of coated BC aggregates, and reveal the influence of non-absorptive coating on BC optical properties. With all geometric elements defined using spheres and overlapping avoided, it becomes possible to use the MSTM to calculate the optical properties of coated BC aggregate, and the MSTM is approximately two orders of magnitude faster than the DDA for particles we consider. Furthermore, the spherical coating shows similar influence on BC optical properties to those with highly complex coating structures. Our results show that the absorption of BC aggregates becomes over two times stronger if they are heavily coated by non-absorptive materials, and the coating also significantly affect the scattering matrix elements. When the coating fraction becomes larger than 0.75, the Rayleigh features of the BC aggregates disappear. We find that the relative position between the coating and aggregates is also a key factor to

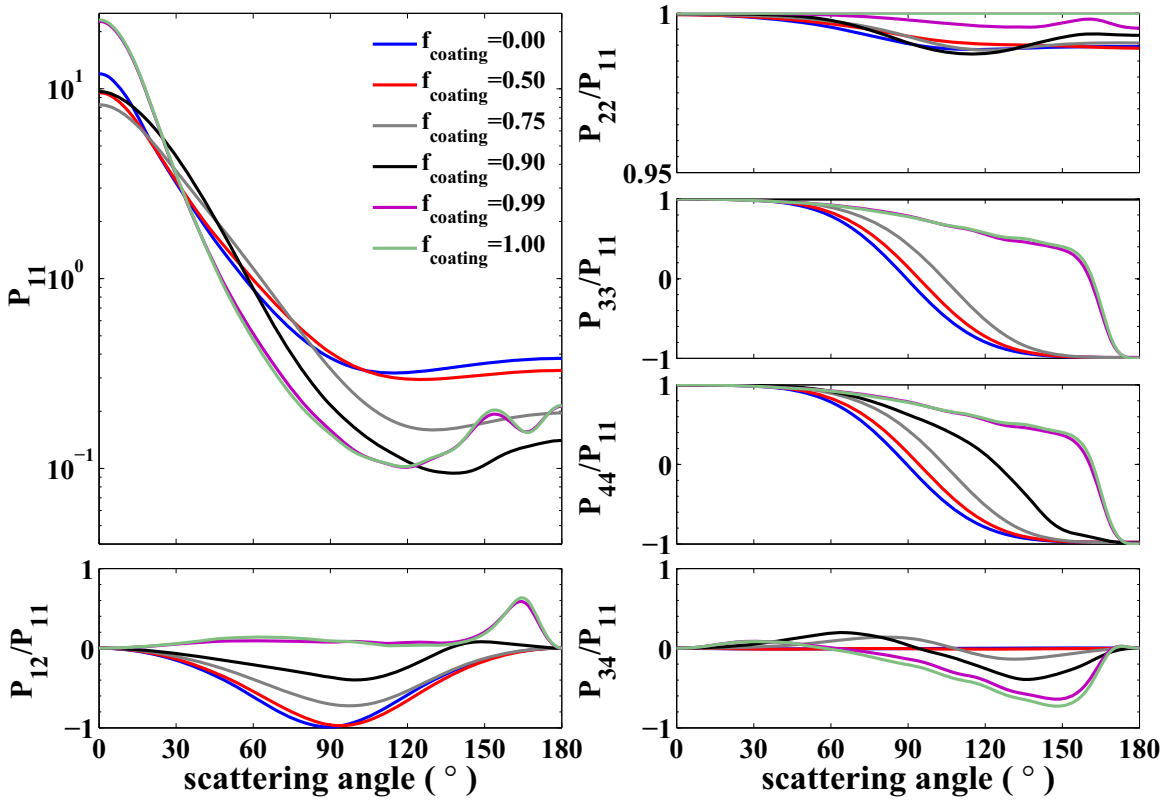

Fig. 9. Same as Fig. 4 but for an ensemble of coated aggregates with a given size distribution.

determine the optical properties of coated aggregates. With the significant influence on BC optical properties, it becomes urgent to consider the coating for BC measurements and radiative simulations. The efficient model developed in this study can play an important role for further applications as a large amount of simulations are needed.

Acknowledgements

We particularly thank Drs. D. M. Mackowski and M. I. Mishchenko for the MSTM code and Drs. M. A. Yurkin and A. G. Hoekstra for the ADDA code. This work was financially supported by the National Natural Science Foundation of China (NSFC) (Grant nos. 41571348, 41505018, 41590873 and 41276181), the National Key Research and Development Program of China (Grant no. 2016YFA0602003), and the Natural Science Foundation of Jiangsu Province (Grant no. BK20150899).

References

[1] Jacobson MZ. Strong radiative heating due to the mixing state of black carbon in atmospheric aerosols. Nature 2001;409:695–697.
[2] Bond TC, Sun H. Can reducing black carbon emissions counteract global warming? Environ Sci Technol 2005;39:5921–5926.
[3] Chakrabarty RK, Moosmüller H, Arnott WP, Garro MA, Tian G, Slowik JG, Cross ES, Han J, Davidovits P, Onasch TB, Worsnop DR. Low fractal dimension cluster-dilute soot aggregates from a premixed flame. Phys Rev Lett 2009;102:235504.
[4] Scarnato BV, Vahidinia S, Richard DT, Kirchstetter TW. Effects of internal mixing and aggregate morphology on optical properties of black carbon using a discrete dipole approximation model. Atmos Chem Phys 2013;13:5089–5101.
[5] Shiraiwa M, Kondo Y, Iwamoto T. Amplification of light absorption of black carbon by organic coating. Aerosol Sci Tech 2010;44:46–54.
[6] Liu D, Allan J, Whitehead J. Ambient black carbon particle hygroscopic properties controlled by mixing state and composition. Atmos Chem Phys 2012;13:2015–2029.
[7] Schnaiter M, Horvath H, Möhler O, Naumann KH, Saathoff H, Schöck OW. UV–vis-NIR spectral optical properties of soot and soot-containing aerosols. J Aerosol Sci 2003;34:1421–1444.
[8] Liu F, Wong C, Snelling DR, Smallwood GJ. Investigation of Absorption and Scattering Properties of Soot Aggregates of Different Fractal Dimension at 532 nm Using RDG and GMM. Aerosol Sci Tech 2013;47:1393–1405.
[9] Liu L, Mishchenko MI. Effects of aggregation on scattering and radiative properties of soot aerosols. J Geophys Res 2005;110:D11211.
[10] Chakrabarty RK, Beres ND, Moosmüller H, China S, Mazzoleni C, Dubey MK, Liu L, Mishchenko MI. Soot superaggregates from flaming wildfires and their direct radiative forcing. Sci Rep 2014;4:5508.
[11] Smith AJA, Peters DM, McPheat R, Lukanihins S, Grainger RG. Measuring black carbon spectral extinction in the visible and infrared. J Geophys Res 2015;120:9670–9683.
[12] Liu F, Smallwood GJ. Radiative properties of numerically generated fractal soot aggregates: the importance of configuration averaging. J Heat Transf 2010;132:207–214.
[13] Liu L, Mishchenko MI. Scattering and radiative properties of complex soot and soot-containing aggregate particles. J Quant Spectrosc Radiat Transf 2007;106(1):262–273.
[14] Smith AJA, Grainger RG. Simplifying the calculation of light scattering properties for black carbon fractal aggregates. Atmos Chem Phys 2014;14:7825–7836.
[15] Martins JV, Artaxo P, Liousse C, Reid JS, Hobbs PV, Kaufman YJ. Effects of black carbon content, particle size, and mixing on light absorption by aerosols from biomass burning in Brazil. J Geophys Res 1998;103:32041–32050.
[16] Wu Y, Cheng TH, Zheng LJ, Chen H. Optical properties of the semi-external mixture composed of sulfate particle and different quantities of soot aggregates. J Quant Spectrosc Radiat Transf 2016;179:139–148.
[17] Shiraiwa M, Kondo Y, Iwamoto T. Amplification of light absorption of black carbon by organic coating. Aerosol Sci Tech 2011;44:46–54.
[18] Zhang R, Khalizov AF, Pagels J, Zhang D, Xue H, Mcmurry PH. Variability in morphology, hygroscopicity, and optical properties of soot aerosols during atmospheric processing. P Natl Acad Sci USA 2008;105:10291–10296.
[19] Bond TC, Habib G, Bergstrom RW. Limitations in the enhancement of visible light absorption due to mixing state. J Geophys Res 2006;111:5025–5030.
[20] Schwarz JP, Gao RS, Spackman JR, Watts LA, Thomson DS, Fahey DW. Measurement of the mixing state, mass, and optical size of individual black carbon particles in urban and biomass burning emissions. Geophys Res Lett 2008;35:337–344.
[21] Smith AJA, Grainger RG. Simplifying the calculation of light scattering properties for black carbon fractal aggregates. Atmos Chem Phys 2014;14:7825–7836.
[22] Li H, Liu C, Bi L, Yang P, Kattawar GW. Numerical accuracy of “equivalent”

spherical approximations for computing ensemble-averaged scattering properties of fractal soot aggregates. J Quant Spectrosc Radiat Transf 2010;111:2127–2132.
[23] Mishchenko MI, Liu L, Mackowski DW. T-matrix modeling of linear depolarization by morphologically complex soot and soot-containing aerosols. J Quant Spectrosc Radiat Transf 2013;123:135–144.
[24] Chung CE, Lee K, Müller D. Effect of internal mixture on black carbon radiative forcing. Tellus B 2012;64:10925.
[25] Dong J, Zhao JM, Liu LH. Morphological effects on the radiative properties of soot aerosols in different internally mixing states with sulfate. J Quant Spectrosc Radiat Transf 2015;165:43–55.
[26] Cheng T, Wu Y, Chen H. Effects of morphology on the radiative properties of internally mixed light absorbing carbon aerosols with different aging status. Opt Express 2014;22:15904–15917.
[27] Liu C, Yin Y, Hu F, Jin H, Sorensen CM. The effects of monomer size distribution on the radiative properties of black carbon aggregates. Aerosol Sci Tech 2015;49:928–940.
[28] Yuan L, Yin Y, Xiao H, Yu X, Hao J, Chen K, Liu C. A closure study of aerosol optical properties at a regional background mountainous site in Eastern China. Sci Total Environ 2016;550:950–960.
[29] Liu F, Yon J, Bescond A. On the radiative properties of soot aggregates-Part 2: effects of coating. J Quant Spectrosc Radiat Transf 2015;172:134–145.
[30] Liu C, Panetta RL, Yang P. The influence of water coating on the optical scattering properties of fractal soot aggregates. Aerosol Sci Tech 2012;46:31–43.
[31] Bergman DJ. The dielectric constant of a composite material—a problem in classical physics. Phys Rep 1978;43:377–407.
[32] Liu C, Chung CE, Zhang F, Yin Y. The colors of biomass burning aerosols in the atmosphere. Sci Rep 2016;6:28267.
[33] Sorensen CM. Light scattering by fractal aggregates: a review. Aerosol Sci Technol 2001;35:648–687.
[34] Filippov AV, Zurita M, Rosner DE. Fractal-like aggregates: relation between morphology and physical properties. J Colloid Interf Sci 2000;229:261–273.
[35] Mishchenko MI, Liu L, Cairns B, Mackowski DW. Optics of water cloud droplets mixed with black-carbon aerosols. Opt Lett 2014;39:2607–2610.
[36] Wu Y, Cheng T, Gu X. The single scattering properties of soot aggregates with concentric core–shell spherical monomers. J Quant Spectrosc Radiat Transf 2014;135:9–19.
[37] Kahnert M, Nousiainen T, Lindqvist H. Models for integrated and differential scattering optical properties of encapsulated light absorbing carbon aggregates. Opt Express 2013;21:7974–7993.
[38] Dlugach JM, Mishchenko MI. Scattering properties of heterogeneous mineral aerosols with absorbing inclussions. J Quant Spectrosc Radiat Transf 2015;162:89–94.
[39] Mackowski DW, Mishchenko MI. Calculation of the T matrix and the scattering matrix for ensembles of spheres. J Opt Soc Am A 1996;13:2266–2278.
[40] Mackowski DW. A general superposition solution for electromagnetic scattering by multiple spherical domains of optically active media. J Quant Spectrosc Radiat Transf 2014;133:264–270.
[41] ⟨http://www.eng.auburn.edu/users/dmckwski/scatcodes/⟩.
[42] Mishchenko MI, Dlugach JM, Yurkin MA, Bi L, Cairns B, Liu L, Panetta LR, Travis L, Yang P, Zakharova N. First-principles modeling of electromagnetic scattering by discrete and discretely heterogeneous random media. Phys Rep 2016;632:1–75.
[43] Yurkin MA, Hoekstra AG. The discrete dipole approximation: an overview and recent developments. J Quant Spectrosc Radiat Transf 2007;106:558–589.
[44] Yurkin MA, Hoekstra AG. The discrete-dipole-approximation code ADDA: capabilities and known limitations. J Quant Spectrosc Radiat Transf 2011;112:2234–2247.
[45] Liu C, Bi L, Panetta RL, Yang P, Yurkin MA. Comparison between the pseudo-spectral time domain method and the discrete dipole approximation for light scattering simulations. Opt Express 2012;20:16763–16776.
[46] Chang H, Charalampopoulos TT. Determination of the wavelength dependence of refractive indices of flame soot. Proc R Soc Lond A 1990;430:577–591.
[47] Li J, Liu C, Yin Y, Kumar KR. Numerical investigation on the Ångström exponent of black carbon aerosol. J Geophys Res 2016;121:3506–3518.
[48] Liu C, Panetta RL, Yang P. Inhomogeneity structure and the applicability of effective medium approximations in calculating light scattering by inhomogeneous particles. J Quant Spectrosc Radiat Transf 2014;146:331–348.